

High-Pressure Dielectric Investigations of Nanocolloidal Aerosil–Nematic Liquid Crystal Composites

Prasad N. Bapat, D. S. Shankar Rao, S. Krishna Prasad,* and C. V. Yelamaggad

Centre for Liquid Crystal Research, Jalahalli, Bangalore 560013, India

Received: July 8, 2010; Revised Manuscript Received: September 7, 2010

We report the effect of applied pressure on the dielectric properties of composites of a nematic liquid crystal with hydrophilic Aerosil particles. The study, which is the first of its kind on the nanocolloidal Aerosil systems, also has the novelty that a weakly polar nematogen is used as the host material. In conjunction with differential scanning calorimetric data, these measurements show that not only $T_{N\text{-}I}$, the nematic–isotropic transition at room pressure, but several other parameters exhibit a nonmonotonic variation with increasing Aerosil concentration. The dependence of the relaxation frequency of the mode connected with the reorientations of the molecules around their short axis is probed along isobaric as well as isothermal paths, and the determined activation parameters are discussed in terms of the chemical structure of the host molecule. The temperature dependence of the relaxation frequency at atmospheric pressure, exhibiting non-Arrhenius behavior, has been analyzed using the Vogel–Fulcher–Tamann expression, yielding information regarding the influence of the Aerosil concentration on the fragility strength as well as the glass transition temperature. The calorimetric data is also discussed in terms of the concept of a crossover from the random-dilution to the random-field limits.

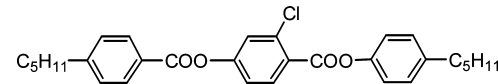
1. Introduction

Liquid crystals in a geometrically confined environment have attracted significant interest in recent times.¹ Such a restriction can be imposed by confining the liquid crystal (LC) in a prefabricated well-defined porous matrix such as Anopore and Nuclepore or an irregular network like aerogels. The consequent disorder can also be realized by having the material in an Aerosil network created by fine (~ 7 nm diameter) silica spheres capped with hydrophilic or hydrophobic agents.² The fragile hydrogen bond network caused by the interactions between the particles in a fluid environment permits the disorder to be created in situ. An important advantage of this network, especially from the viewpoint of this study, is that by simply varying the concentration of the silica particles the resulting random disorder can be controlled and fine-tuned. The composites of Aerosils with LC exhibit gelation, which at low concentrations of Aerosil act as soft gels.³ At atmospheric pressure, a variety of probes, including dielectric spectroscopy, have been used^{4–11} to understand the behavior of LC–Aerosil dispersions. Recently,¹² we reported pressure–temperature phase diagrams of LC–Aerosil composite system formed with a strongly polar nematogen. Despite this strong interest on the behavior of these composites, there has been no report on the effect of high pressure on their dielectric properties. Here we describe the results of the first such investigation on the pure nematogen and its nanocolloidal composites with Aerosil, in the soft gel regime.

2. Experimental Section

The molecular structure of the liquid crystalline compound, PCPBB, used for the investigation is given below:

It exhibits the isotropic–nematic (I–N) transition at 121.8 °C and the N phase can be supercooled to subambient temperatures. The dielectric anisotropy $\epsilon_a = \epsilon_{||} - \epsilon_{\perp}$ (where $\epsilon_{||}$



and ϵ_{\perp} stand for the dielectric constants along and perpendicular to the director, respectively) of PCPBB changes from positive to negative at a certain frequency, or in other words, a dual frequency characteristic,¹³ a feature that we have not probed in this work. To be noted is the feature that the PCPBB molecule does not have a strongly polar terminal group, unlike the well-studied cyanobiphenyl system. It has, of course, two ester groups and a chlorine atom in the meta position, all of which contribute to the dipole moment in the lateral direction. However, for the properties of interest here the strength of the polarity of the system is the manifestation of the effective dipole moments in terms of the dielectric constants $\epsilon_{||}$ and ϵ_{\perp} . For PCPBB these values are 10 and 6 respectively, which may be compared with the values of 18 and 6.5 for the well-known strongly polar molecule, pentylcyanobiphenyl.¹⁴ Now let us recall the scenario discussed by earlier authors for the LC molecules in Aerosil dispersions.² The high density of the silanol groups on the surface of the Aerosil particles causes them to have a hydrophilic character. The particles can bind with one another by means of the intermolecular hydrogen bonds through the Si–O–H groups present at the surface. When the liquid crystal molecules and the Aerosil particles coexist as a dispersion, then such bonding leads to the formation of a random gel. If the interaction between the surface of the Aerosil particles and the liquid crystalline molecules is significant then two contradictory influences can develop: the presence of the nonliquid crystalline Aerosil particles reduces the orientational order in the LC medium and if the interface between the Aerosil and the liquid crystal formed is of proper type then it could promote the orientational order at least at the surface. A consequent possible LC-material dependent scenario is that in molecules such as the cyanobiphenyls the strongly polar terminal cyano group would like to be normal to the silica surface (perhaps reinforced by the

* To whom correspondence should be addressed. E-mail: skpras@gmail.com

hydrogen bonding between the nitrile group of LC and the hydroxyl of silanol) and therefore the induced order would tend to minimize, at least in the soft-gel regime, the disorder due to the presence of foreign particles. On the other hand, in systems not possessing a strongly polar terminal group, such as PCPBB, the surface-induced order could be significantly small and the disorder due to the presence of the Aerosil particles dominates the properties. These features are expected to influence the dielectric behavior. The composites were prepared using hydrophilic Aerosil particles (Aerosil 300, Degussa Corp.) with a diameter of ~ 7 nm,¹⁵ and employing the solvent mixing procedure. Known amounts of the degassed and dried (at a temperature of ~ 200 °C) Aerosil particles were added to a weighed quantity of PCPBB contained in pure acetone. The solution was sonicated for about 1 h to obtain a good dispersion of the Aerosil in the medium and kept at a temperature of 55 °C over a period of 15 h, for the evaporation of acetone. The sample was then kept under vacuum for 24 h to ensure complete evaporation of acetone, with the temperature maintained at 110 °C. The absence of agglomerations in thin films of the prepared mixtures when viewed under a polarizing microscope is an indication of the uniform dispersion of the particles. Aerosil mixtures are usually characterized in terms of the Aerosil density defined as $\rho_a = m_a/V_{LC}$, where m_a is the mass of Aerosil and V_{LC} is the volume of the liquid crystal. Since the density of the LC is ≈ 1 g cm⁻³, ρ_a can be written as just m_a/m_{LC} . Investigations have been carried out on mixtures with $\rho_a = 0.015, 0.03, 0.06$, and 0.11 g cm⁻³ (we drop the units hereafter) as well as on pure PCPBB.

We will recall briefly the details of the high-pressure dielectric cell employed, given elsewhere.¹⁶ It is a modified form of the optical cell used in our laboratory^{17a} and very similar to the one used earlier for the study of ferroelectric liquid crystals.^{17b} Essentially, it consists of the sample contained in a PET gasket (thickness ~ 0.06 mm) sandwiched between two steel cylinders, which also serve as electrodes, and enclosed in an elastomer tube. The elastomer tube also serves to prevent contamination of the sample by the pressure transmitting fluid (Plexol). Care was taken to make sure that the sample assembly was electrically isolated from the rest of the high-pressure setup. The surface of the steel cylinders in contact with the sample was pretreated with a silane solution to promote homeotropic alignment of the LC molecules. Screws threaded into the steel cylinders established electrical contact between the sample and the measuring equipment. The sample temperature was sensed by a K-type thermocouple and measured using a digital multimeter (Keithley DMM 2000) to a precision of ± 10 mK. In this setup, the sample pressure is the same as that in the plumbing line and thus could be conveniently measured with a high precision (± 3 bar) Heise gauge. The dielectric parameters were determined in the frequency range 100 Hz to 1 MHz with the help of an impedance analyzer (HP4194A). The interfacing of the multimeter and the impedance analyzer to a PC enabled the data acquisition process to be automated by a program written in Visual Basic. Owing to the construction geometry, a shortcoming of this high-pressure cell is that the gasket used to contain the sample is also present in the active area of the electrodes, adding its own contribution to the measured capacitance of the sample that cannot be

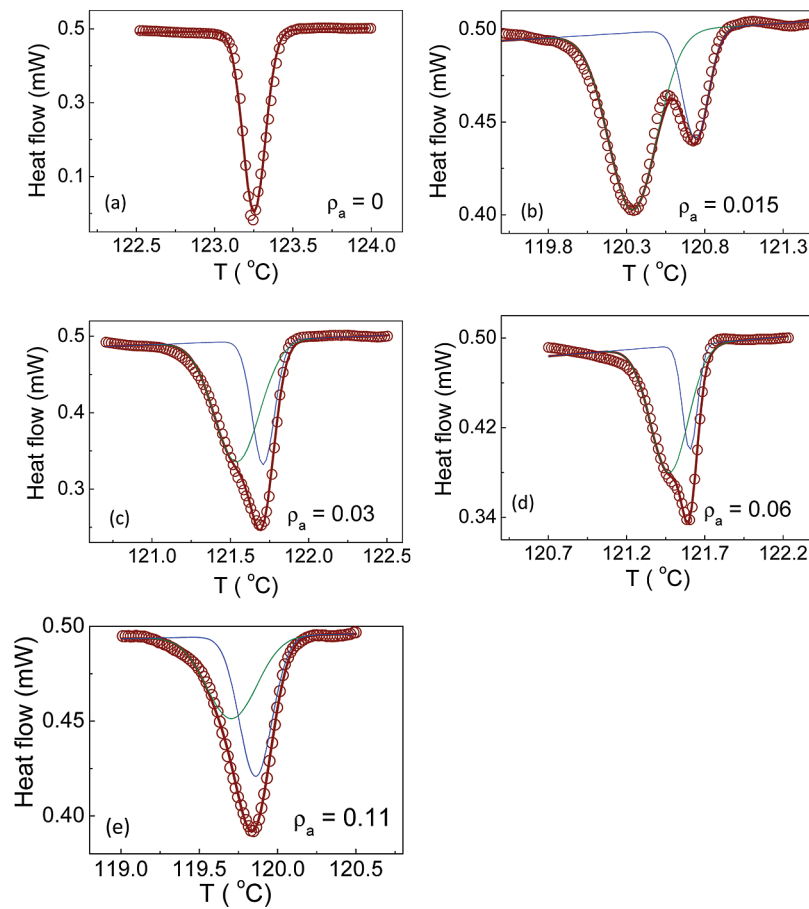


Figure 1. Differential scanning calorimetric scans obtained on cooling for PCPBB (a) and its Aerosil composites (b–e) in the vicinity of the nematic–isotropic transition. The thick lines represent a fit to a linear term for the background, plus one or two Gaussian terms. The individual contributions of the latter are shown as thin lines, in the case of composites.

determined exactly. The calculation of the actual dielectric constant is thus not feasible, and therefore we discuss the dielectric results in terms of the capacitance C' and $C'' = C' \times D$ (D being the loss factor), representing the real and imaginary parts of the dielectric constant. The experiments were always conducted along isobars and in the cooling mode, i.e., keeping the pressure constant at any desired value and decreasing the sample temperature at a constant rate of ~ 1 °C/min from the required temperature. Differential scanning calorimetric measurements were done with a Perkin-Elmer Diamond DSC at a rate of 1 °C/min.

3. Results and Discussion

3.1. Differential Scanning Calorimetry. Figure 1 shows the DSC scans across the N–I transition for PCPBB and the four different composites. The point to be highlighted in these scans is that, while a single peak is observed for the bulk sample and the $\rho_a = 0.11$ mixture, the other composites show a twin-peak profile, a feature that is particularly clear for $\rho_a = 0.015$. Even on a qualitative level, it is seen that the separation between the twin peaks decreases as ρ_a increases, with the two peaks merging into a single broad one for the $\rho_a = 0.11$ composite. For quantitative description of the DSC profile, the data was fit to an equation which is a sum of a linear background term, and either one or two Gaussians terms, for the single- or double-peak case. As seen in Figure 1, the quality of the fitting to such an expression is very good in the peak region for all the cases, but not so good in the tail region for some mixtures (for the $\rho_a = 0.11$ mixture, although visual inspection data suggests a single peak, a slightly better goodness of fitting was obtained with two Gaussian terms). The fitting yielded the transition temperature T_{NI} , taken as the high-temperature peak value; T_{RFC} , the temperature of the second peak, when present; ΔT , the difference in the two peak temperatures; and ΔH_{NI} and ΔH_{RFC} , the corresponding transition enthalpy contributions, taken as the area under the peaks. The dependence of these parameters on the Aerosil concentration, displayed in Figure 2, brings out the nonmonotonic dependence on ρ_a for T_{NI} , a feature now well-known,^{4,7} but also for T_{RFC} and the two ΔH values.

The double-peak profile in calorimetric studies on LC–Aerosil systems was first observed in high-resolution ac calorimetric measurements^{4,18,19} and subsequently in DSC experiments,¹¹ a feature that assumes significance for the following reason. Based on the studies on alkyl/alkoxy cyanobiphenyl–Aerosil mixtures, composites with $\rho_a < 0.1$ are classified as soft gels, and those with $\rho_a \geq 0.1$ as stiff gels. We will apply the same criterion for the present mixtures also. In the soft gel region, the density of Aerosil particles exceeds the “gelation” (percolation) threshold, and consequently a network is formed by diffusion-limited aggregation through hydrogen bonding of the silica spheres. The gel is soft owing to the fact that the links among the silica particles can easily break. It may be mentioned that rheological studies in this region have shown that the Aerosil composites exhibit soft glass behavior, generally seen for materials such as foams, emulsions, particulate suspensions, and slurries.³ More importantly, specific heat measurements have shown that these soft gels exhibit two weakly first-order specific heat peaks in the N–I coexistence region. Combining high-resolution calorimetric, light scattering, and microscopy techniques, Caggioni et al.¹⁸ propose that in the LC–Aerosil systems the nematic order develops from the isotropic phase through a two-step process and can be understood in terms of a system exhibiting temperature-dependent disorder strength. They argue that the N–I transition with weak quenched random disorder proceeds

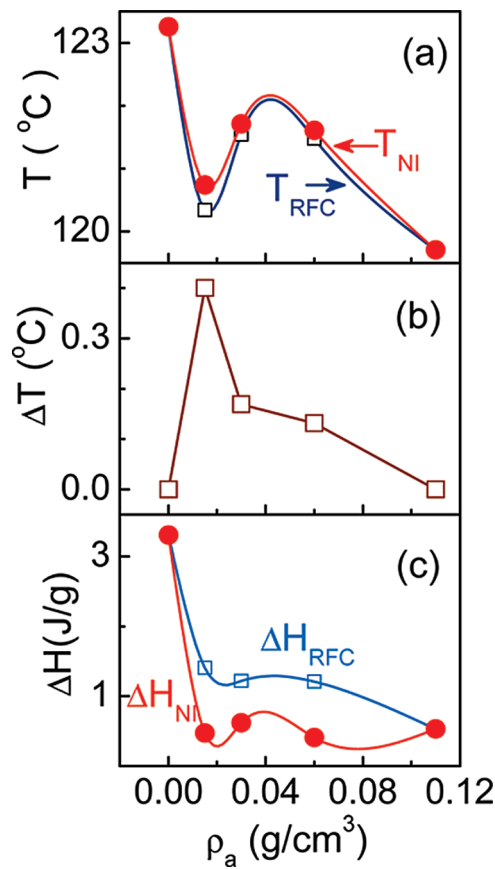


Figure 2. Aerosil-concentration dependence of (a) the transition temperatures, (b) the difference in the peak temperatures of the twin peak profile shown in Figure 1, and (c) the corresponding transition enthalpies. In (a) and (c), the error bars obtained from the fitting are smaller than the symbol size used. See text for details regarding the notation RFC and NI. The lines serve only as guides to the eye.

via such a two-step process, due to a crossover (referred to as RFC in this article) from a random-dilution regime where the silica gel couples to the scalar part of the nematic order parameter, to a low-temperature random-field regime where the coupling induces distortions in the director field. Such a crossover phenomenon has been studied in disordered antiferromagnets.²⁰ It should be noted that the high-temperature peak is much sharper (and has a lower enthalpy of transition) compared to the low-temperature peak, a behavior that was observed in another LC–Aerosil system also,¹¹ and can be explained since the high-temperature region is associated with the appearance of the domains from the isotropic phase, having a weak coupling to the Aerosil network. The coupling becomes stronger across the range where the second peak is seen, thus broadening the peak. The combined value of $\Delta H_{RFC} + \Delta H_{NI}$ is smaller by $\sim 45\%$ for the Aerosil case ($\rho_a = 0.015$) than the ΔH for the bulk, suggesting that the transition becomes weaker in the presence of even a small quenched disorder. Further, the high-temperature process, associated with the random dilution limit, has 2–3 times smaller ΔH value than the one connected with the RFC region. Several theoretical attempts, based on the effect of the network on the nematic orientational order parameter, have been made to explain the nonmonotonic variation of T_{NI} in Aerosil mixtures.^{4,21} But as discussed by us in previous articles,^{10,11} none of the models gives a satisfactory reproduction of the experimental data. Perhaps, the drawback is that none of them invoke any mechanism which can bring in a nonmonotonic variation of the quenched disorder when the concentration of the Aerosil particles is monotonically changed.

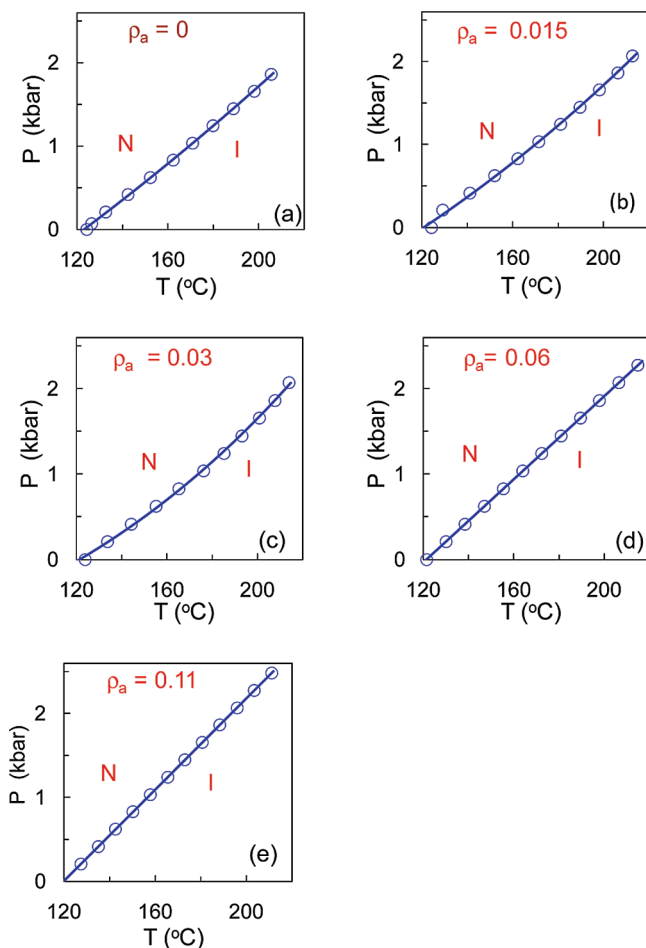


Figure 3. Influence of pressure on the N–I phase boundary for pure PCPBB and the Aerosil composites. The line through the symbols represents the fit to the Simon–Glatzel equation (eq 2).

3.2. Pressure–Temperature Phase Diagram. The effect of pressure on the N–I boundary, obtained using an optical transmission method, for all the five materials—pure compound and the four composites—is shown in Figures 3a–e. The data appears smooth over the entire range of pressure studied for the composites, in particular, a clear indication that the network remains intact even at elevated pressures and therefore the data is suitable for quantitative analysis. The pressure dependence of the transition temperature of a first-order transition (as is the case for the N–I transition) is very well described by the classical Clausius–Clapeyron equation

$$\frac{dT}{dP} = T \frac{\Delta V}{\Delta H} \quad (1)$$

If the transition volume ΔV and the transition enthalpy ΔH are considered to be independent of pressure, and are given by their values at atmospheric pressure, then eq 1, which results in a linear relationship (with a slope $m = dT/dP$) between the transition temperature and transition pressure, can be used to describe the phase boundary. A more general expression, especially successful in describing melting transition in a variety of materials (including liquid crystals), is the Simon–Glatzel equation²²

$$\frac{P}{A} = \left(\frac{T}{T_0} \right)^n - 1 \quad (2)$$

TABLE 1: Parameters Obtained by Fitting the P – T Phase Boundary to Simon–Glatzel Equation (Eq 2)

ρ_a (g/cm ³)	A (kbar)	T_0 (°C)	n
0	4.21 ± 0.03	123.3 ± 0.004	$1.94 \pm 1 \times 10^{-4}$
0.015	2.59 ± 0.05	120.7 ± 0.02	$2.77 \pm 4 \times 10^{-4}$
0.03	1.55 ± 0.03	121.7 ± 0.01	$4.0 \pm 4 \times 10^{-4}$
0.06	$9.63 \pm 1 \times 10^{-7}$	$121.6 \pm 2 \times 10^{-10}$	$1.0 \pm 1 \times 10^{-10}$
0.11	$10.69 \pm 1 \times 10^{-7}$	$119.9 \pm 3 \times 10^{-10}$	$1.0 \pm 1 \times 10^{-10}$

which contains only two material-dependent constants, A and n (in the form used here the reference pressure P_0 is taken as room pressure and therefore T_0 corresponds to T_{NI} at room pressure). The coefficients A , T_0 , and n determined by fitting the data for all the materials studied here are shown in Table 1. While it is not difficult to get these coefficients from such a fit, a proper determination of the errors associated is not trivial since eq 2 is transcendental in nature. Therefore, we followed the method suggested by Babb²³ in which the errors on A and n are determined by performing the fitting while one of them is held fixed. The exponent n obtained shows a nonmonotonic behavior, although the values are much higher for the composites. With the slope (m , determined by fitting a straight line to the data) and transition enthalpy values at room pressure, and making an approximation that the deviation from a linear variation of the transition temperature with pressure is not large, the Clausius–Clapeyron equation can be employed to calculate the volume change at the transition. Employing the combined ΔH_{NI} and ΔH_{RFC} values obtained from DSC measurements, we determined the transition volumes. The ρ_a dependences of the

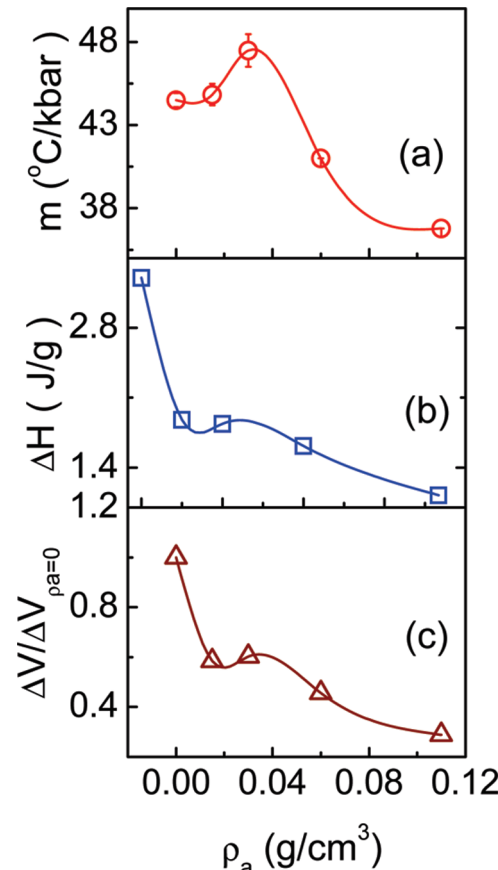


Figure 4. Variation of (a) the slope of the P – T boundary determined at atmospheric pressure, (b) the total enthalpy ($\Delta H_{NI} + \Delta H_{RFC}$), and (c) the transition volume determined from the Clausius–Clapeyron equation (eq 1), normalized with respect to that for pure PCPBB, on the concentration of Aerosil. The lines are merely guide to the eye.

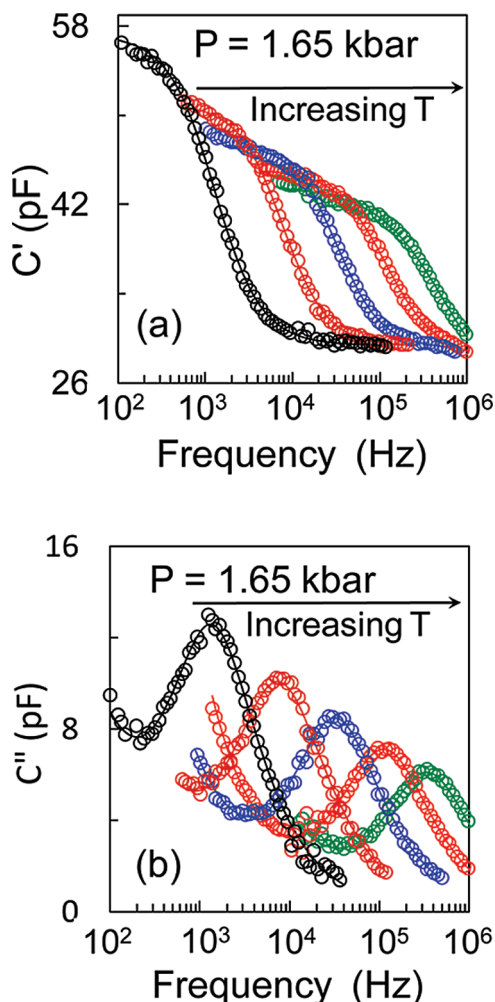


Figure 5. Spectroscopic profiles of the complex capacitance at a fixed pressure of 1.65 kbar in the nematic phase for temperatures in steps of 20 °C over the range 140–60 °C (from right to left) of a representative composite ($\rho_a = 0.03$) shown as the (a) real part and (b) imaginary part. The lines are the fit to the Havriliak–Negami equation (eq 4).

slope and the combined ΔH and ΔV (normalized with respect to ΔV for $\rho_a = 0$) are shown in Figure 4. All these parameters again exhibit the feature that varying the concentration of Aerosil does not affect their magnitude in a monotonic fashion.

3.3. Dielectric Measurements. 3.3.1. Frequency Spectrum. The frequency dependence of C' and C'' for different temperatures in the N phase of a representative Aerosil composite ($\rho_a = 0.03$) at a fixed pressure are shown in Figure 5, a and b, respectively; similar plots for different pressures at a constant temperature of 90 °C are given in Figure 6, a and b. A feature that is seen in all the profiles is that there is a conductivity tail at low frequencies and a clear dielectric relaxation at each temperature and pressure. Considering the frequency range at which the relaxation occurs, as well as the room pressure measurements with excellent homeotropic alignment of the molecules, the process is attributed to the rotations of the molecules about the short molecular axis. On a qualitative level, it is observed that for the data set at constant temperature, the frequency at which the profile has a maximum in C'' , taken to be a measure of the relaxation frequency, f_R , decreases with increasing pressure. On the other hand, at constant pressure, f_R decreases when the temperature is decreased. These two features are compatible with the fact that the thermodynamic path traversed will increase the orientational ordering in the medium. To quantitatively extract f_R and C_R , the strength of the mode,

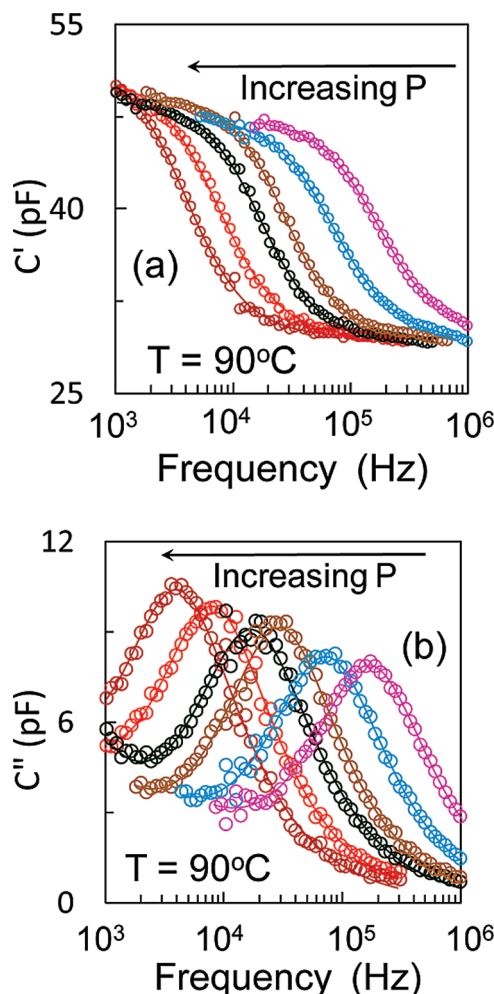


Figure 6. Isothermal ($T = 90$ °C) spectroscopic profiles of the complex capacitance for pressures in steps of 0.42 kbar over the range 0.41–2.48 kbar (from right to left) in the nematic phase of a representative composite ($\rho_a = 0.03$) shown as the (a) real part and (b) imaginary part. The lines are the fit to the Havriliak–Negami equation (eq 4).

the raw C' vs f and C'' vs f (the measuring frequency) data were fit to the standard Havriliak–Negami equation²⁴

$$C^*(f) = C_\infty + \frac{C_R}{[1 + (if/f_R)^\alpha]^\beta} \quad (3)$$

To account for the dc conductivity contribution to the imaginary part of the capacitance, a term proportional to $1/f$ was added to the right-hand side of eq 3. Throughout the entire range of measurement for all the samples, only a single relaxation was seen and the profiles could be very well described by a Debye relaxation ($\alpha, \beta \approx 1$ in eq 3), as seen in Figure 6, a and b.

3.3.2. Activation Parameters. The temperature variation of f_R in the N phase for two representative materials, $\rho_a = 0$ and $\rho_a = 0.06$, for different set values of pressures are given in Figures 7 and 8. Similar, but isothermal, data as a function of pressure are shown in Figures 9 and 10. The temperature dependence of the relaxation frequency associated with the director mode in the nematic phase (a fluid) can be expected to be described by the Arrhenius expression with an activation energy ΔE

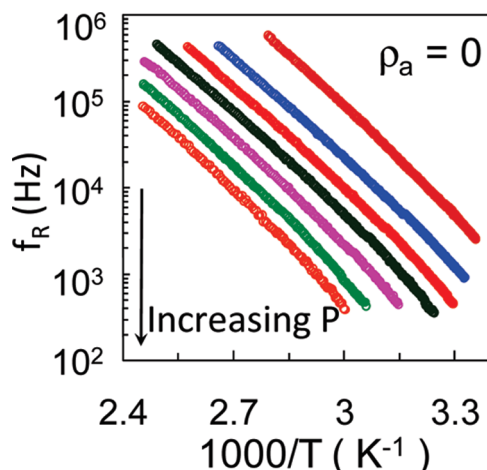


Figure 7. Semilogarithmic plot of the temperature dependence of the relaxation frequency versus inverse temperature at different pressures for PCPBB. The different sets correspond to data obtained in steps of 0.41 kbar from room pressure to 2.48 kbar, starting from the top.

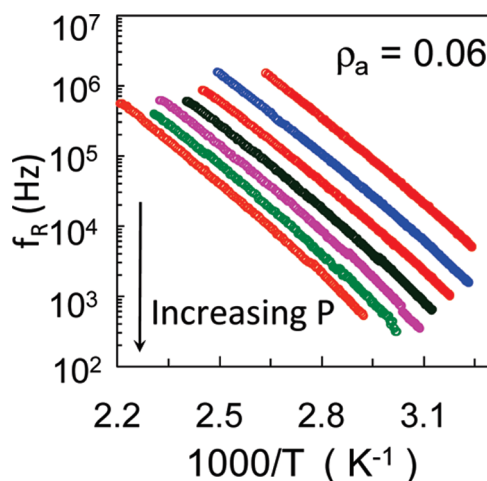


Figure 8. Semilogarithmic plot of the temperature dependence of the relaxation frequency versus inverse temperature at different pressures for the $\rho_a = 0.06$ composite. The different sets correspond to data obtained in steps of 0.41 kbar from room pressure to 2.48 kbar, starting from the top.

This equation, according to which $\log(f_R)$ should vary linearly with $1/T$, has been widely used in liquid crystal literature. However, as can be seen from Figures 7 and 8, at least in quite a few cases, there is a noticeable nonlinearity in the data. Such nonlinear behavior has been described in the literature in terms of vitrification of the sample.²⁵ With the high-pressure cell employed, the absence of a subambient temperature facility combined with the fact that the sample, being thick, had a greater tendency for crystallization prevented us from collecting data over a much larger temperature range (especially at low temperatures) than depicted in figures 7 and 8 required for such an analysis. Therefore, we analyze the high-pressure data in terms of the Arrhenius behavior. The pressure and temperature dependences of the relaxation frequency are governed by two activation parameters,^{26,27} activation enthalpy ΔH_a and activation volume ΔV_a . (In the literature the terms activation energy and activation enthalpy are sometimes interchangeably used. While their mathematical forms are the same, the former is defined at constant volume, and the latter at constant pressure.) These parameters are given by

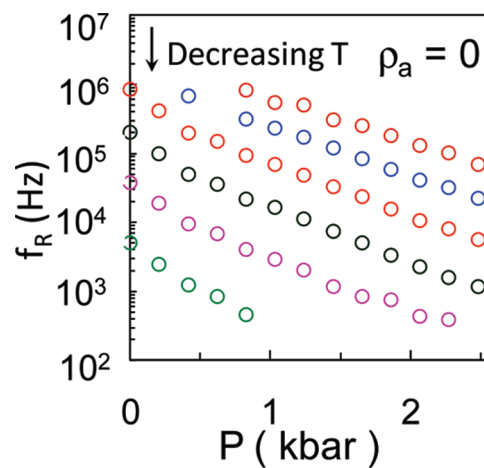


Figure 9. Semilogarithmic plot of the pressure dependence of the relaxation frequency at different temperatures in the N phase of PCPBB. The different sets correspond to data obtained at intervals of 20 °C from 130 to 30 °C, starting from the top.

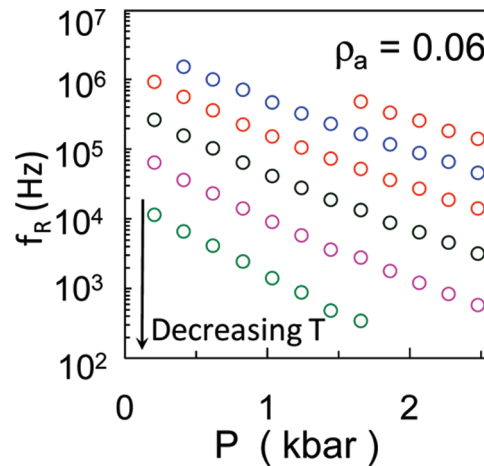


Figure 10. Semilogarithmic plot of the pressure dependence of the relaxation frequency at different temperatures in the N phase for the $\rho_a = 0.06$ composite. The different sets correspond to data obtained at intervals of 20 °C from 150 to 50 °C, starting from the top.

$$f_R(T) = f_0 \exp\left(\frac{\Delta E}{k_B T}\right) \quad (4)$$

$$\Delta H_a = RT(\partial \ln \tau / \partial T^{-1})_p \quad (5)$$

$$\Delta V_a = RT(\partial \ln \tau / \partial p)_T \quad (6)$$

where the relaxation time is given by $\tau = 1/2\pi f_R$. The isobaric and isothermal f_R data, such as those shown in Figures 7–10, have been fitted to eqs 5 and 6, respectively. Figure 11, a and b, shows the pressure and temperature dependences of the two activation parameters for $\rho_a = 0$ and 0.06 samples. Both samples behave in a similar fashion, viz., ΔH_a increases linearly with increasing pressure, ΔV_a decreases drastically with increasing temperature in a manner that can be described by an exponential decay function. Generally, ΔV_a has been reported^{16,26,27} to be decreasing with increasing temperature, but not as strongly as in the present case. The activation volume is considered as the free volume that the molecule must have in order to perform the rotational jump over the potential barrier and thus can be expected to decrease with increasing temperature. The fact that in the present experiments the steep variation with temperature happens only at low temperatures perhaps suggests the influence

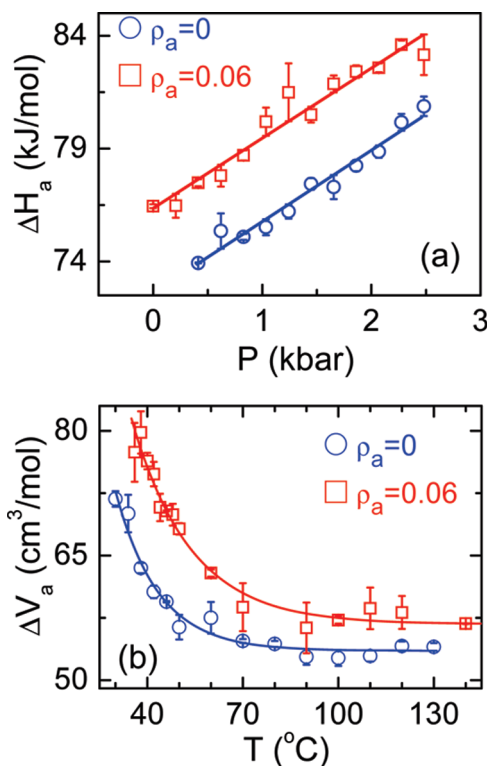


Figure 11. (a) Pressure dependence of the activation enthalpy and (b) temperature dependence of the activation volume in the N phase of pure PCPBB (circles) and the $\rho_a = 0.06$ composite (squares). The lines are merely guides to the eye. Notice that at any given pressure (temperature) the activation values are higher for the composite.

of possible glass behavior. ΔH_a has been seen^{16,27,29} to show either a decrease or increase as pressure is increased, with perhaps dimerization of the molecules, especially in compounds with a strongly polar terminal group, playing an important role. In the present studies, the host material has a weakly polar group (chlorine), but attached to the meta position of a phenyl ring. Further, polar groups at such positions are not known to promote dimer formation. Since the effect of high pressure on the dielectric behavior of such weakly polar nematogens has hardly been investigated, it is difficult to generalize the feature. However, keeping in mind that even in situations of strongly polar compounds disfavoring the dimers a very weak decrease or a slight increase of ΔH_a with pressure is seen,¹⁶ the behavior observed may be general for all nondimer cases. The fact that, at any given pressure, the activation enthalpy is higher for the Aerosil composite indicates that the potential barrier could be influenced by the fragile network also, with the basic behavior being still dominated by the host material, as suggested by the data sets for the two materials ($\rho_a = 0$ and 0.06) being essentially parallel to each other over the entire pressure range.

3.3.3. Glassy Behavior. The super-Arrhenius behavior, commonly seen in glass-forming molecular liquids and polymeric systems, is often represented by the Vogel–Fulcher–Tammann (VFT) expression. The VFT equation expresses the relaxation time τ ($= 1/2\pi f_R$) in a form that is similar to the Arrhenius equation, but with the important exception that it diverges exponentially at a finite temperature. In the frequency regime, it is expressed as

$$f_R(T) = f_0 \exp\left(\frac{DT_0}{T - T_0}\right) \quad (7)$$

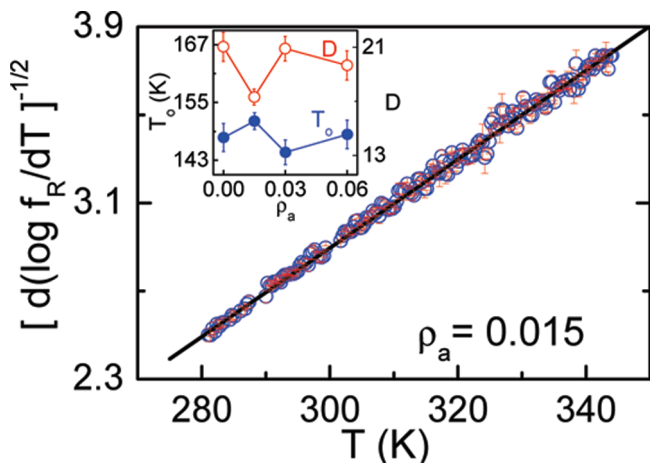


Figure 12. Data at atmospheric pressure for a representative material ($\rho_a = 0.015$ composite) showing the fit (the solid line) of the temperature derivative of the relaxation frequency to the linearized form of the Vogel–Fulcher–Tammann (VFT) equation (eq 8). The inset displays the VFT temperature T_0 and the fragility constant D for different concentrations of Aerosil.

Here D is the fragility strength coefficient and T_0 is the VFT estimate of the glass transition temperature. Considering the nonlinear nature of this expression, Stickel et al.³⁰ suggested the following linearized form of it by derivitizing the equation with respect to T .

$$\left(\frac{d \log(f_R)}{dT}\right)^{-1/2} = (DT_0)^{-1/2}(T - T_0) \quad (8)$$

which is a linear equation where the parameters D and T_0 can be directly obtained from the slope and intercept. It may be noted that, when the intercept is zero, the Arrhenius behavior results. In the case of PCPBB as well as its composites, a thin sample could be supercooled well below ambient. Thus, we could extend the relaxation frequency measurements at atmospheric pressure using thin samples sandwiched between two ITO-coated glass plates to the subambient region with the help of a Peltier cooling system. In these studies, the minimum temperature at which the data could be collected was dictated by crystallization of the sample (in the range of 6–10 °C). With the help of such a data, the derivative analysis mentioned above was performed. For all the samples, the representation as in eq 8 was linear in T , aiding the determination of the parameters D and T_0 . Figure 12 shows a representative data set exhibiting the linear dependence of the left-hand side of eq 8, and the inset depicts the Aerosil concentration dependence of these parameters. The magnitudes of the D values observed indicate that the materials are quite fragile glass-formers. Further, it is surprising to see the nonmonotonic dependence (although modest) of D and T_0 on ρ_a , like many other material parameters that we have discussed in this article.

In summary, we have performed the first high-pressure dielectric measurements on a nanocolloidal system comprising a weakly polar nematic liquid crystal and its composites with Aerosil particles in the soft gel regime. Differential scanning calorimetric measurements carried out on several concentrations bring out in clear terms the double-peak profile for gels in the soft gel regime. The appearance of such a double-peak profile is associated with processes wherein the network establishes a coupling with the order parameter to begin with, but ultimately introduces distortions on the

director field itself. Peak profile analysis of the calorimetric scans has helped extraction of thermal parameters connected with these two regimes, and highlights the fact that not only the temperature but the transition enthalpy describing the two processes also undergoes a nonmonotonic variation with Aerosil concentration. An interesting finding of this study is that the pressure–temperature phase diagrams in conjunction with the above-mentioned calorimetric data bring out the fact that the slope of the phase boundary and the volume jump across the nematic–isotropic transition also possess this nonmonotonic behavior. Further, determination of the dielectric relaxation frequency as a function of temperature and pressure reveals that the dynamics of the system remains intact even in the gels at atmospheric as well as elevated pressures, and that the activation volume decreases exponentially with temperature for the pure liquid crystal as well as for gels, with the absolute value being lower for the latter case. Detailed analysis of the temperature dependence of the relaxation frequency connected with the short axis flipping of the nematic director employing the Vogel–Fulcher–Tamann expression characteristic of non-Arrhenius behavior yields useful information regarding the influence of the Aerosil concentration on the fragility strength as well as the glass transition temperature. The observation of the nonmonotonic dependence of many parameters on the Aerosil concentration, should be an impetus to carry out theoretical work to explain such features.

References and Notes

- (1) For reviews on this topic, see: Crawford, G. P., Zumer, S., Eds. *Liquid Crystals in Complex Geometries*; Taylor and Francis: London, 1996. Krishna Prasad, S.; Shankar Rao, D. S.; Nair, G. G. *J. Indian Inst. Sci.* **2009**, *89*, 211–227.
- (2) For reviews see: Iannacchione, G. S. *Fluid Phase Equilib.* **2004**, 222–223, 177. Popa-Nita, V.; Gerlic, I.; Kralj, S. *Int. J. Mol. Sci.* **2009**, *10*, 3971–4008.
- (3) Bandyopadhyay, R.; Liang, D.; Colby, R. H.; Harden, J. L.; Leheny, R. L. *Phys. Rev. Lett.* **2005**, *94*, 107801-1–4.
- (4) Iannacchione, G. S.; Garland, C. W.; Mang, J. T.; Rieker, T. P. *Phys. Rev. E* **1998**, *58*, 5966–5981.
- (5) Marinelli, M.; Ghosh, A. K.; Mercuri, F. *Phys. Rev. E* **2001**, *63*, 061713-1–9.
- (6) Kutnjak, Z.; Kralj, S.; Zumer, S. *Phys. Rev. E* **2002**, *66*, 041702-1–8.
- (7) Ramazanoglu, M.; Larochelle, S.; Garland, C. W.; Birgeneau, R. J. *Phys. Rev. E* **2008**, *77*, 031702-1–10.
- (8) Bellini, T.; Clark, N. A.; Degiorgio, V.; Mantegazza, F.; Natale, G. *Phys. Rev. E* **1998**, *57*, 2996–3006.
- (9) Jin, T.; Finotello, D. *Phys. Rev. Lett.* **2001**, *86*, 818–821.
- (10) Lobo, C. V.; Krishna Prasad, S.; Yelamaggad, C. V. *J. Phys.: Condens. Matter* **2006**, *18*, 767–776.
- (11) Jayalakshmi, V.; Nair, G. G.; Krishna Prasad, S. *J. Phys.: Condens. Matter* **2007**, *19*, 226213-1–12.
- (12) Bapat, P. N.; Shankar Rao, D. S.; Krishna Prasad, S. *Thermochim. Acta* **2009**, *495*, 115–119.
- (13) Hegde, G.; Nair, G. G.; Krishna Prasad, S.; Yelamaggad, C. V. *J. Appl. Phys.* **2005**, *97*, 093105-1–6. Chandrasekhar, S.; Raja, V. N.; Krishna Prasad, S.; Shankar Rao, D. S. *Mol. Cryst. Liq. Cryst.* **2004**, *410*, 359–368. Schadt, M. *Appl. Phys. Lett.* **1982**, *41*, 692–699.
- (14) Ratna, B. R.; Shashidhar, R. *Mol. Cryst. Liq. Cryst.* **1977**, *42*, 113–125.
- (15) The Aerosil samples were kindly given to us by Mr. Vikas Rane of d-hindia Ltd, Mumbai.
- (16) Sandhya, K. L.; Shankar Rao, D. S.; Krishna Prasad, S.; Hiremath, U. S.; Yelamaggad, C. V. *Thermochim. Acta* **2007**, *452*, 65–70.
- (17) (a) Krishna Prasad, S.; Shankar Rao, D. S.; Jeyagopal, P. *Phys. Rev. E* **2001**, *64*, 011706-1–4. Gupta, V. K.; Shankar Rao, D. S.; Lobo, C. V.; Krishna Prasad, S. *Thermochim. Acta* **2006**, *440*, 205–211. (b) Krishna Prasad, S.; Khened, S. M.; Chandrasekhar, S. *Ferroelectrics* **1993**, *147*, 351–365.
- (18) Caggioni, M.; Roshi, A.; Barjami, S.; Mantegazza, F.; Iannacchione, G. S.; Bellini, T. *Phys. Rev. Lett.* **2004**, *93*, 127801-1–4.
- (19) Marinelli, M.; Mercuri, M.; Paoloni, S.; Zammit, U. *Phys. Rev. Lett.* **2005**, *95*, 237801-1–4.
- (20) See e.g.: Belanger, D. P. *Braz. J. Phys.* **2000**, *30*, 682–692.
- (21) Hourri, A.; Jamee, P.; Bose, T. K.; Thoen, J. *Liq. Cryst.* **2002**, *29*, 459–466.
- (22) Simon, F. E.; Glatzel, G. Z. *Anorg. Allg. Chem.* **1929**, *178*, 309. Also see: Salter, L. *Philos. Mag.* **1954**, *45*, 369–378.
- (23) Babb, S. E., Jr. *Rev. Mod. Phys.* **1963**, *35*, 400–413.
- (24) Havriliak, S.; Negami, S. *J. Polym. Sci., Part C: Polym. Symp.* **1966**, *14*, 99–117.
- (25) A good summary of the present understanding of the glass transitions can be seen in: Hecksher, T.; Nielsen, A. I.; Olsen, N. B.; Dyre, J. C. *Nat. Phys.* **2008**, *4*, 737–741. McKenna, G. B. *Nat. Phys.* **2008**, *4*, 673.
- (26) Naoki, M.; Endou, H.; Matsumoto, K. *J. Phys. Chem.* **1987**, *91*, 4169–4174.
- (27) Sandmann, M.; Busing, D.; Bruckert, T.; Wurflinger, A.; Urban, S.; Gestblom, B. *SPIE* **1998**, *3318*, 223.
- (28) See e.g.: Roland, C. M.; Psurek, T.; Pawlus, S.; Paluch, M. *J. Polym. Sci.: Part B: Polym. Phys.* **2003**, *41*, 3047–3052.
- (29) Urban, S.; Wurflinger, A. In *Nonlinear Dielectric Phenomena in Complex liquids*; Rzoska, S. J., Zhelezny, V. P., Eds.; Kluwer: Dordrecht, The Netherlands, 2004; pp 211–220.
- (30) Stickel, F.; Fischer, E. W.; Richert, R. *J. Chem. Phys.* **1995**, *102*, 6251–7. This derivative form of analysis has recently been revisited by: Drozd Rzoska, A. *J. Chem. Phys.* **2009**, *130*, 234910-1–8.

JP106318E